Relative Channel Reciprocity Calibration in MIMO/TDD Systems

Florian KALTENBERGER[1], Haiyong JIANG[1,3],
Maxime GUILLAUD[2], Raymond KNOPP[1]

[1]*EURECOM Institute, 2229 route des Crêtes, B.P. 193, 06904 Sophia Antipolis, France*
{Florian.Kaltenberger,Haiyong.Jiang,Raymond.Knopp}@eurecom.fr

[2]*Vienna University of Technology, Institute of Communications and Radio-Frequency Engineering, Gußhausstraße 25/389, 1040 Wien, Austria,* guillaud@tuwien.ac.at

[3]*Infineon Technologies France, 2600 route des Crêtes, 06560 Sophia Antipolis, France*

Abstract: Channel state information at the transmitter (CSIT) can greatly improve the capacity of a wireless MIMO communication system. In a time division duplex (TDD) system CSIT can be obtained by exploiting the reciprocity of the wireless channel. This however requires calibration of the radio frequency (RF) chains of the receiver and the transmitter, which are in general not reciprocal. In this paper we investigate different methods for relative calibration in the presence of frequency offsets between transmitter and receiver. We show results of theses calibration methods with real two-directional channel measurements, which were performed using the Eurecom MIMO Openair Sounder (EMOS). We demonstrate that in a single-user MIMO channel and for low signal-to-noise (SNR) ratios, the relative calibration method can increase the capacity close to the theoretical limit.

1. Introduction

In a wireless communication system using antenna arrays, channel state information at the transmitter (CSIT) can greatly improve the capacity of the wireless link. This gain becomes even more significant in multi-user MIMO systems. CSIT can be acquired in several ways. In time division duplex (TDD) systems, the physical forward and the backward channel are reciprocal since they operate on the same carrier frequency [1]. In reality however, the communication channel does not only consist of the physical channel, but also the antennas, RF mixers, filters, A/D converters, etc., which are not necessarily identical for all devices. Therefore the system needs to be calibrated before channel reciprocity can be exploited.

Contrarily to absolute calibration [2] where external reference sources are used to measure and compensate for the imperfections of each RF chain independently, we focus here on approaches relying on relative calibration [3, 4]. In this context, the calibration relies on the devices exchanging channel measurements, rather than on extra hardware.

Relative calibration can be formulated as a total least squares (TLS) problem either in the time domain [3] or in the frequency domain [4]. Efficient solutions exist for a couple of special cases, such as SIMO or MISO [3] or when the reciprocity matrices are assumed to be diagonal (which is equivalent to having negligible cross-talk between the different RF chains) [4]. In this paper we include the effect of frequency offsets in the reciprocity model and investigate their effect on the relative calibration. For the analysis in this paper we use real two-directional channel measurements, which were performed using the Eurecom MIMO Openair Sounder (EMOS) [5].

2. Reciprocity model

The investigated reciprocity model is based on the technique introduced in [3], whereby the characteristics of the amplifiers at the transmitter and receiver are modeled with linear time-invariant filters. Compared to [3] the model presented in this section also contains the effects of up- and down-conversion and is thus able to model frequency offsets between transmitter and receiver.

Let us consider a point-to-point TDD communications system involving two devices denoted A and B. Denote the number of antennas at side A and B with N_A and N_B respectively. As depicted in Fig. 1, the channel as seen by transceivers in the digital domain, is comprised of the effective electromagnetic channel ($C(t)$), assumed identical in both directions, and filters modeling the imperfections of the power amplifiers (T_A, T_B) and low-noise amplifiers (R_A, R_B). In the case where antenna arrays are used, those are vector-input, vector-output filters.

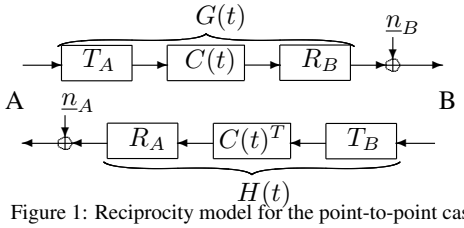

Figure 1: Reciprocity model for the point-to-point case

In the ideal case, often considered in the literature, T_A, T_B, R_A and R_B are all identity filters and carrier frequency at both sides are identical. In that case, the channels are perfectly reciprocal without requiring calibration. Conversely, we investigate practical methods applying to non-ideal cases. As the notations imply, the filters modeling the amplifiers (T_A, T_B, R_A, R_B) are assumed to remain constant over the observed time horizon. Let f_A and f'_A denote the up-conversion and down-conversion frequencies at side A, and f_B and f'_B the up- and down-conversion frequencies at node B. It is very likely that $f_A = f'_A$ and $f_B = f'_B$ since the mixers are normally driven by the same clock. However, f_A can differ significantly from f_B, typically by up to one kHz.

For a given frequency f, the channel impulse response as measured by the digital signal processor is the cascade of the up-conversion, the transmit filter, the electromagnetic channel, the receive filter, and the the down-conversion. The measured uplink and downlink channel are thus modeled as:

$$G(t,f) = R_B(f)e^{2\pi j f'_B t}C(t,f)T_A(f)e^{-2\pi j f_A t}, \quad (1)$$

$$H(t,f) = R_A(f)e^{2\pi j f'_A t}C(t,f)^T T_B(f)e^{-2\pi j f_B t}. \quad (2)$$

Note that in the sequel, we will omit the dependency on f, although it should be kept in mind that that the flat-fading models used below hold independently for each frequency, in typical OFDM fashion.

In the time domain, a similar set of equations is obtained by replacing products by convolutions and matrices by linear filters in the Eqs. (1) and (2).

Departing from classical calibration techniques whereby T_A, T_B, R_A and R_B are estimated and compensated individually, [3] introduced the concept of *relative* calibration. It consists in introducing the filters $P_A = R_A^{-T}T_A$ and $P_B = T_B^T R_B^{-1}$. Eliminating C from Eqs. (1) and (2), one obtains

$$(G(t)e^{-2\pi j(f_A - f'_B)t}) = P_B^{-1}(H(t)^T P_A e^{-2\pi j(f_B - f'_A)t}). \quad (3)$$

$f_A - f'_B$ and $f_B - f'_A$ are residual frequency offset in the channel estimations of both directions. The frequency offsets can be estimated using several consecutive channel estimates of $G(t)$ and $H(t)$. The problem is equivalent to the one of estimating the frequency of a single complex sinusoid in noise-corrupted discrete-time samples. One efficient solution is proposed in [6]. Once $f_A - f'_B$ and $f_B - f'_A$ are estimated, we compensate each channel measurements which eliminates the effect of frequency offset, for the following derivation, we can omit the frequency offset and use the similar notation as in [4]

$$G(t) = P_B^{-1} H(t)^T P_A. \tag{4}$$

In the considered point-to-point scenario, relative calibration consists in estimating directly P_A and P_B, using eq. (4) and the measured values of $G(t)$ and $H(t)$. Once these are known, the channel can be estimated through reciprocity using (4).

2.1 Design of reciprocity estimators for the point-to-point case

Let us consider a series of K bi-directional channel measurements, i.e. both $G(t)$ and $H(t)$ are assumed to be measured simultaneously (or with negligible time difference) at times t_i, $i = 1 \dots K$. We wish to design an estimator for (P_A, P_B) based on the noisy channel measurements $(\hat{G}(t_i), \hat{H}(t_i))$, $i = 1 \dots K$. Considering one single frequency, and dropping the index f for notational simplicity, the following estimator minimizes the objective function suggested by the reciprocity relationship $P_B G(t) - H(t)^T P_A = 0$. Since this relationship only applies to the true channels, we allow for compensation terms $\tilde{G}(t)$ and $\tilde{H}(t)$ to be added to $\hat{G}(t)$ and $\hat{H}(t)$, in the spirit of the Total Least-Squares (TLS) technique [7], in order to account for the uncertainty due to the estimation noise:

$$(\hat{P}_A, \hat{P}_B) = \underset{\substack{(P_A, P_B, \tilde{G}_i, \tilde{H}_i), \\ \text{s.t.} ||P_A||_2^2 = 1}}{\operatorname{argmin}} \sum_{i=1}^{K} \left|\left| P_B \left(\hat{G}(t_i) + \tilde{G}_i \right) - \left(\hat{H}(t_i) + \tilde{H}_i \right)^T P_A \right|\right|_2^2 + \left|\left| \tilde{G}_i \right|\right|_2^2 + \left|\left| \tilde{H}_i \right|\right|_2^2. \tag{5}$$

It can be seen from eq. (5) that if the compensation terms $\tilde{G}$ and $\tilde{H}$ are exactly equal to the measurement noise, the first norm vanishes. The condition $||P_A||_2^2 = 1$ ensures that the trivial solution $(P_A, P_B) = (0, 0)$ is avoided. This condition is added without loss of generality since the set of parameters (P_A, P_B) is over-determined: it can be seen from eq (4) that the family of solutions where P_A and P_B are multiplied with the same scalar factor indeed represents a single solution to the problem at hand.

2.2 Extension to multiple users

The generalization of the above model to the case of multiple users is straightforward. Here we address the point-to-multipoint case, which has practical implications in cellular networks. Let us assume that device A is involved in multiple bidirectional TDD communications with N devices denoted $B_1 \dots B_N$ (in the context of cellular communications, A can be understood as the base station, while B_n are the mobile nodes in the cell). Denoting by T_{B_n} and R_{B_n} the respective gains of transmit and receive RF subsystems of device n, the measured channels between A and B_n are

$$G_n(t) = R_{B_n} C_n(t) T_A, \quad \text{and} \quad H_n(t) = R_A C_n(t)^T T_{B_n}. \tag{6}$$

Denoting $P_{B_n} = T_{B_n}^T R_{B_n}^{-1}$, we have as before $G_n(t) = P_{B_n}^{-1} H_n(t)^T P_A$. Note that T_A, R_A are common to all links, while T_{B_n}, R_{B_n} are specific to each node B_n. The estimator for the multi-user case is a generalization of (5) and given by

$$(\hat{P}_A, \hat{P}_{B_1} \dots \hat{P}_{B_N}) = \underset{\substack{(P_A, P_{Bn}, \tilde{G}_{n,i}, \tilde{H}_{n,i}) \\ \text{s.t.} ||P_A||_2^2 = 1}}{\operatorname{argmin}} \sum_{\substack{n=1\dots N \\ i=1\dots K}} \left|\left| P_{Bi} \left(\hat{G}_n(t_i) + \tilde{G}_{n,i} \right) - \left(\hat{H}_n(t_i) + \tilde{H}_{n,i} \right)^T P_A \right|\right|_2^2 + \left|\left| \tilde{G}_{n,i} \right|\right|_2^2 + \left|\left| \tilde{H}_{n,i} \right|\right|_2^2 . \tag{7}$$

3. Approaches to solve the minimization problem

The quartic (note e.g. the product between P_B and $\tilde{G}_i$, which are both components of the variable under optimization) objective function defined in (5) makes the solution of the optimization problem non trivial. For relatively small problem sizes, this is solvable by standard non-convex optimization methods, although the complexity currently prevents any real-time exploitation. Another avenue to reduce the complexity of the considered estimation problem is to simplify the model above.

3.1 Frequency-flat SISO case

In the SISO case, the filters P_A and P_B are scalars and thus the products in (4) commute. Letting $P = P_B^{-1} P_A$ yields $G(t) = H(t)P$. Since both $G(t)$ and $H(t)$ are affected by estimation errors, the estimate of P can be estimated as the classical total least-squares solution: collecting K pairs of measurements in the vectors $\hat{\mathbf{g}} = [\hat{G}(t_1), \dots, \hat{G}(t_K)]^T$ and $\hat{\mathbf{h}} = [\hat{H}(t_1), \dots, \hat{H}(t_K)]^T$, $\hat{P}$ is estimated as

$$\underset{\tilde{\mathbf{h}}, \tilde{\mathbf{g}}, P}{\operatorname{argmin}} ||\tilde{\mathbf{h}}||_2^2 + ||\tilde{\mathbf{g}}||_2^2 \quad \text{s.t.} \quad (\hat{\mathbf{h}} + \tilde{\mathbf{h}})P = (\hat{\mathbf{g}} + \tilde{\mathbf{g}}). \tag{8}$$

This TLS problem can be easily solved using the classical solution based on the singular value decomposition (SVD) [8].

3.2 MIMO with Diagonal Reciprocity Matrices

The model of eqs. (1) and (2) incorporates cross-talk between all antenna pairs in an array. In reality, the effect of this phenomenon is negligible, making P_A and P_B diagonal. This decouples the MIMO problem (4) into $N_A N_B$ SISO problems

$$[G(t)]_{i,j} = [P_B^{-1}]_{i,i} [H(t)]_{j,i} [P_A]_{j,j}, \tag{9}$$

which are solved as in Section 3.1.

3.3 Frequency-selective SISO case

The case of the frequency selective channel is not conceptually different from the flat-fading problem, except for the added complexity due to the increased dimensions. Two approaches can be envisioned:

1. A per-subband approach, in which the reciprocity estimator is applied independently to each subband, i.e.,

$$G(t, f) = H(t, f)P(f). \tag{10}$$

The complexity of this approach scales linearly with the transmission bandwidth, however it fails to exploit the correlation across subbands between the reciprocity parameters. This correlation is expected to be high, since the impulse responses of P_A and P_B are expected to be extremely short in practice.

2. Estimating the reciprocity parameters in the time domain by transforming (10) into the time domain:

$$G(t,\tau) = H(t,\tau) * P(\tau), \tag{11}$$

Under the assumption that $P(\tau)$ is a FIR filter such that $P_B(\tau) * P(\tau) = P_A(\tau)$, a solution to this problem is proposed in [3], based on the deconvolution algorithm of [9].

Those two approaches outlined above are compared in Section 4. with simulation and Section 5. over real measured data.

3.4 MIMO with diagonal matrix at one side

The nonzero non-diagonal elements in the matrices P_A and P_B are mainly caused by the crosstalk between antennas. We assume here that P_B is diagonal. This is a reasonable simplification for the systems like cellular networks. Because the eNodeBs are less resource-constrained and the antennas can be placed far enough form each other, thus avoiding the crosstalk. The whole estimation process can be split into a MISO calibration and a TLS problem.

In the first step we estimate P_B using the similar technique proposed in [10]. In the second step we estimate P_A, by substituting the estimated P_B from step 1 in Equation (4). We have again a TLS problem where now only P_A remains unknown.

Strictly speaking, this TLS problem slightly violates the assumption of a standard TLS problem [8]. Since after P_B being estimated, we have: $G(t) = (\hat{P}_B^{-1} H(t)^T)\, P_A$ The noise in the matrix $(P_B^{-1}\hat{H}(t)^T)$ is $(P_B^{-1}\tilde{H}(t)^T)$, whose covariance matrix is diagonal but not a identity matrix. However, numerical simulation shows this effect is negligible.

4. Accuracy and Complexity Comparison

In this section, we compare the numerical performance of the two methods envisioned in Section 3.3.

Method 1: Consider the estimation of one $P(f)$ from $K = 20$ channel estimations for each subcarrier(N_c in total). The main part of computation is to find the right singular vectors of a N_c by 2 matrix $[\hat{g}, \hat{h}]$ [8], which are also the right eigenvectors of a 2 by 2 matrix $[\hat{g}, \hat{h}]^H \cdot [\hat{g}, \hat{h}]$. The latter can be calculated analytically and requires $8K$ complex multiplications/additions, and a few other operations. Thus the complexity of estimating all the subcarriers is around $\mathcal{O}(K \cdot N_c)$

Method 2: Essentially, this method constructs a STLS (Structured Total Least Square) problem and uses numerical computation to solve a LS (Least Square) problem within each iteration. According to the fast algorithm provided in [9], it takes $(M_1 \cdot M_2)$ flops to solve an M_1 by M_2 LS problem. So in our case, the complexity will be $\mathcal{O}(L_p \cdot L_{\text{ch}} \cdot K \cdot N_{\text{iter}})$ FLOPS (real floating point operations, multiplication or addition), where L_p is the length of the impulse response of the reciprocity filter $P(t)$, L_{ch} is the length of the channel impulse response, N_{rl} is the number of estimations we use for

the estimator, and N_{iter} stands for the average number of iterations. Fig. 2 shows the average complexity while setting the stop criterion to 10^{-5} and 10^{-7} .

For the evaluation of the accuracy comparison, we perform a Monte Carlo simulation consisting 1000 runs. The 2 methods are then applied to estimate the reciprocity $P(f)$ and $P(\tau)$ in frequency and time domain respectively. As another comparison of Method 2, a frequency domain filter which nulls out the non-used subband is applied upon the estimation result of the FIR filter $P(\tau)$. The relative errors defined by $\frac{\|\hat{P}(f)-P(f)\|^2}{\|P(f)\|^2}$ are briefly shown in Fig. 2 and 3. It can be seen in Fig. 3 that the performance curve of the unfiltered time domain estimate turns flat in high SNR because the influence of the filter dominates the relative error. It's obvious that despite of close accuracy, the estimator in frequency domain significantly outperform its counterpart in time domain in the aspect of complexity.

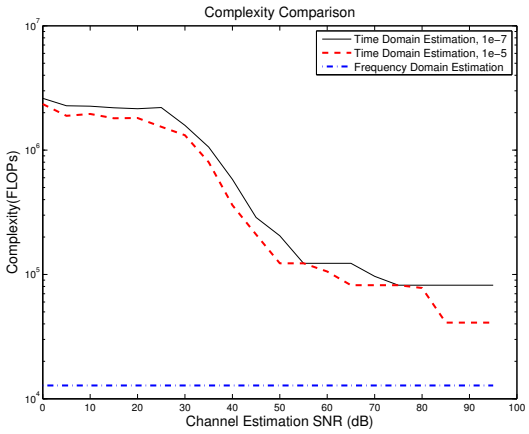

Figure 2: Complexity

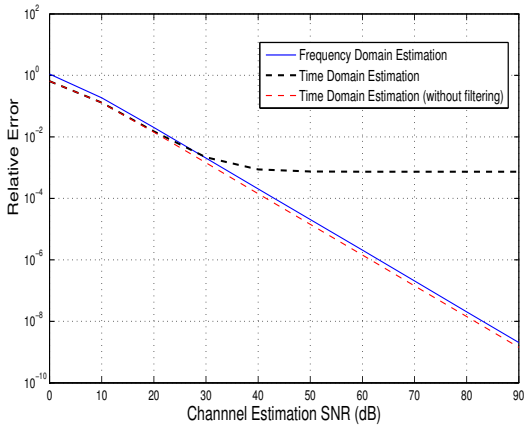

Figure 3: Accuracy Comparison

5. Experimental validation

5.1 Description of the Channel Measurements

The measurements were conducted with the Eurecom MIMO Openair Sounder (EMOS) [5]. The EMOS is a stripped-down version of the Eurecom OpenAirInterface.org platform that transmits additional pilot symbols instead of the scheduled access channels. It can be configured for multi-user and two-way channel sounding. The current EMOS hardware consists of laptop computers with Eurecom's dual-RF data acquisition cards and two clip-on 3G Panorama antennas. The cards operate at 1.900–1.920 GHz with 5 MHz channels[1]. For the evaluations we use a measurement taken in the Eurecom laboratory, were both nodes are stationary and in the same room. The parameters of the measurement system are summarized in Table 1.

The EMOS uses an orthogonal frequency division multiplexing (OFDM) modulated sounding sequence with 256 subcarriers (out of which 160 are non-zero) and a cyclic prefix length of 64. One frame is 64 OFDM symbols (2.667 ms) long and is divided in a downlink (DL) transmission time interval (TTI) and an uplink (UL) TTI of equal length. Each TTI contains 10 pilot symbols, whose subcarriers are multiplexed over

[1]Eurecom has a frequency allocation for experimentation around its premises.

Parameter	Value
Center Frequency	1917.6 MHz
Sampling Rate	6.5 MHz
FFT size	256
Number of Subcarriers (Q)	160
Useful Bandwidth	4.0625 MHz
Max. Transmit Power	20 dBm
Number of Antennas (M)	2
Frame length (UL and DL)	2.667 ms

Table 1: Parameters of the Eurecom MIMO OpenAir Sounder (EMOS).

the transmit antennas to ensure orthogonality in the spatial domain. The pilot symbols are used at the other end for channel estimation.

For the two-way measurements, one node is configured as a base station (BS) and one node as a user terminal (UT). The UT synchronizes to the BS over the air using the transitted synchronization sequence. Synchronization is verified by decoding the transmitted broadcast channel. The UT estimates the DL while the BS estimates the UL. We therefore get one two-directional channel estimate every frame. Both nodes store their estimates to disk. Since the BS also transmits a frame number using its broadcast channel, the measurements can be aligned in a post-processing step.

The EMOS channel estimation procedure consists of two steps. Firstly, the pilot symbols are derotated with respect to the first pilot symbol to compensate the frequency offset within one TTI. Note however, that there is still a frequency offset between estimates between frames. Secondly, the pilot symbols are averaged to increase the measurement SNR. The channel is then estimated in the frequency domain by multiplication of the derotated and averaged symbols with the complex conjugate of the pilot symbol.

The frequency offsets between the transmitter and the receiver can be in the order of a few 100 Hz and neglecting them yields unusable results. In this paper we propose two methods to solve this problem.

The first approach is to compensate the residual frequency offset in the raw channel measurement data before reciprocity estimation. As described in Section 2., the frequency offset can be estimated estimated from the evolution of the phase of several consecutive channel estimates of G(t) and H(t). We use the solution based on the weighted average of the phase differenced is proposed in [6]. The estimated frequency offset is then compensated by multiplying the channel estimates with a complex exponential with the negative estimated frequency offset. Finally we use the basic reciprocity formula (10) to estimate the reciprocity matrices.

In the case when the time-variation of the physical channel is much less than the frequency offsets of the cards, a second approach is based on the fact that the phase drifts are exactly antipodal in the uplink and the downlink and therefore the uplink and downlink can be modeled as conjugates of each other:

$$G(t, f) = H(t, f)^* \, P(f). \tag{12}$$

Note that, strictly speaking, this model only applies to strictly constant channels, for which exploiting reciprocity is of little use. In (12), the complex conjugate operation $(\cdot^*)$ models the fact that phase drifts occurring with opposite signs are observed at nodes A and B. In that case, the above model enables seamless frequency offset compensation.

In this paper both of the two approach are applied and the results are compared in Section 5.3

5.2 Performance Metrics

The metric adopted here to evaluate the quality of the estimation of the reciprocal channel is the gain in channel capacity. Assume that we want to transmit from A to B over the channel G. We can distinguish three cases, depending on whether perfect, partial, or no channel state information is available at the transmitter (CSIT). For each case we evaluate the maximum achievable mutual information:

1. G is known only at B: the best is to choose the transmit covariance matrix $R_{\mathrm{Tx}} = I$. The capacity is classically $C_1 = \sum_i \log_2 \left(1 + \frac{E_S}{N_A N_0}\lambda_i\right)$, where λ_i are the eigenvalues of GG^H and E_S/N_0 the SNR.

2. G is known to A and B: $C_2 = \sum_i \log_2 \left(1 + \frac{E_S \gamma_i}{N_A N_0}\lambda_i\right)$, where the γ_i are obtained from the waterpouring algorithm [11].

3. A has only knowledge of G_{est} (estimated from the reciprocity matrices) and B knows G. We assume that we use the same transmission scheme as in case 2, but the transmit covariance $R_{\mathrm{Tx,est}}$ is calculated from G_{est} instead of G. $C_3 = \log_2 \det \left(I + \frac{E_S}{N_A N_0} G R_{\mathrm{Tx,est}} G^H\right)$.

5.3 Results

In this section we show feasibility of the reciprocity estimation using the channel measurements described in Section 5.. We show results for wideband MIMO channels with diagonal reciprocity matrices. Further we compare the method using frequency offset compensation with the simplified method for stationary channels.

For the analysis in this paper, the measurements were split in blocks of approximately 200 frames each. The reciprocity matrices $P(f)$ were estimated using the first 20 consecutive frames of a block. Subsequently we use these estimates to calculate the downlink channel from the uplink channel for the rest of the frames based on (12) or (10) (according whether frequency offset compensation is applied).

In the case of MIMO channel, where diagonal reciprocity matrices are assumed, the MIMO problem is decoupled in a series of SISO problems (cf. Section 3.2). We thus estimate the reciprocity filters in the frequency domain using the SVD-based TLS solution from [8] per subcarrier (cf. Section 3.1).

First we show results for the method using frequency offset compensation and reciprocity estimation according to the model (4). The average frequency offset in the measurement has been estimated to be $-536.5\,\mathrm{Hz}$. In Fig. 4 we plot the ergodic (mean) capacity for different values of SNR, for the three cases outlined in Section 5.2. It can be seen that for high SNR the capacity of with and without CSIT become very similar, so obviously here hardly any performance improvements are possible. However, for low SNR, the channel knowledge obtained by the reciprocity estimation brings some gain. If we look closer at the low SNR case in Fig. 5, where we plot the CDF of C_1, C_2, and C_3 for an SNR of $10\,\mathrm{dB}$ using all the subcarriers and all the frames as samples, it can be seen that that for this case large performance gains are possible.

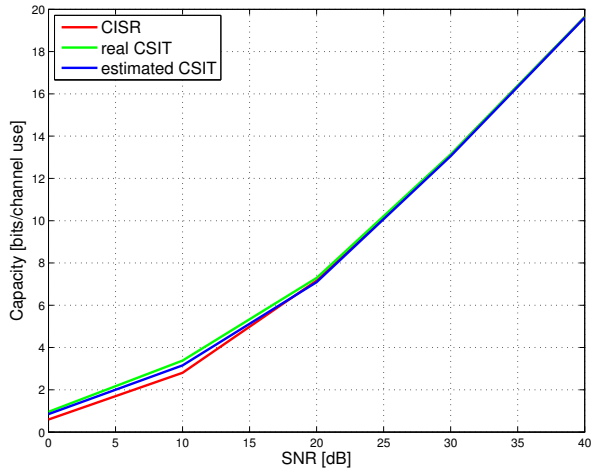

Figure 4: Ergodic capacity with frequency offset compensation. "CSIR"=no CSIT assumed, "real CSIT"=genie-aided perfect channel knowledge at Tx, "estimated CSIT"=CSIT according to (4).

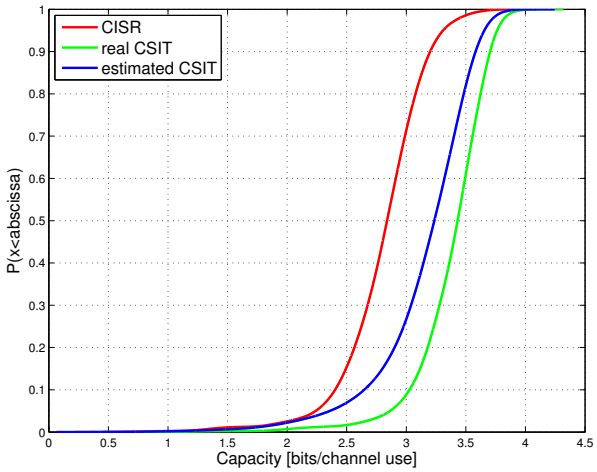

Figure 5: Capacity CDF at 10 dB SNR with frequency offset compensation. "CSIR"=no CSIT assumed, "real CSIT"=genie-aided perfect channel knowledge at Tx, "estimated CSIT"=CSIT according to (4).

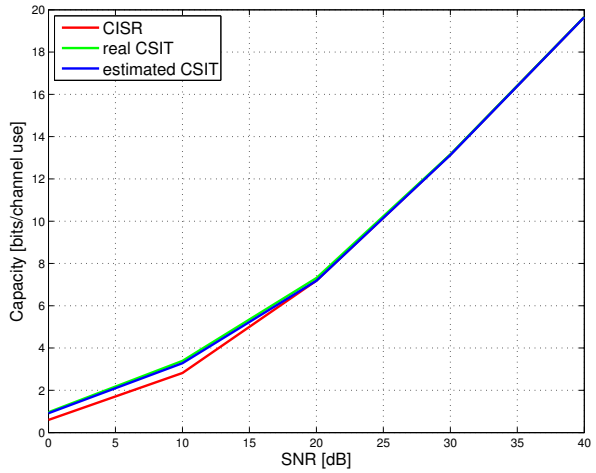

Figure 6: Ergodic capacity *without* frequency offset compensation."CSIR"=no CSIT assumed, "real CSIT"=genie-aided perfect channel knowledge at Tx, "estimated CSIT"=CSIT according to (12).

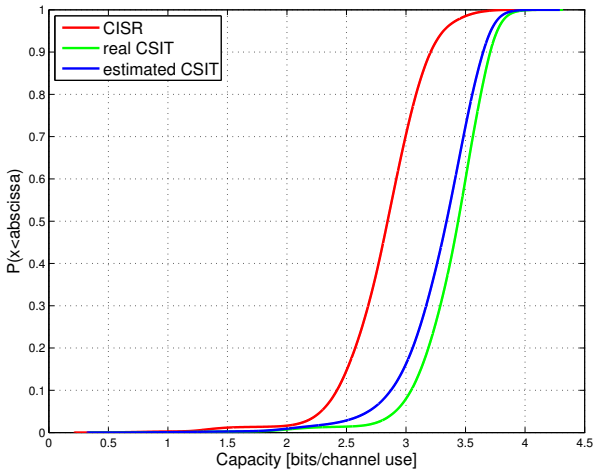

Figure 7: CDF of the capacity at 10 dB SNR *without* frequency offset compensation. "CSIR"=no CSIT assumed, "real CSIT"=genie-aided perfect CSIT, "estimated CSIT"=CSIT according to (12).

Secondly we show results for the method that uses the conjugate of the channel in the uplink and does not apply any frequency offset compensation (cf. Section 5.1). Fig. 6 and Fig. 7 again show the ergodic capacity for increasing SNR values and the CDF of the capacity for an SNR of 10 dB. It can be seen that this method actually performs even better than the method that compensates the frequency offsets. However, it has to be noted that this method will not work in the presence of faster time-variation of the physical channel.

6. Conclusions

In this paper we have shown how to practically exploit channel reciprocity in a MIMO TDD system in order to obtain channel state information at the transmitter. We have verified the method using real two-way MIMO channel measurements that were conducted using the Eurecom MIMO Openair Sounder (EMOS). It was shown that

the method is able to increase the capacity of a single-user MIMO system close to the theoretical limit.

The channel measurements used in this paper are synchronized over the air as in a real system. This kind of synchronization results in frequency offsets since the clocks at the two nodes are not identical. The frequency can be compensated using standard methods, but residual frequency offsets will always remain. While these residual offsets might not have an impact on standard receiver design, they do have a big impact on the exploitation of channel reciprocity, since even the smallest offset of a few Hz will accumulate and make the UL and DL channels non-reciprocal within a few seconds. In the case of stationary measurements this problem can be avoided by modeling the uplink and downlink as complex conjugates.

Future work thus has to focus on channel reciprocity methods in the presence of frequency offsets and time-varying channels. Also we would like to test the method on the multi-user MIMO case, where even higher increase in capacity can be expected.

Acknowledgments

Part of this work was performed while Maxime Guillaud was with FTW. FTW's research is supported in part by the COMET competence center program of the Austrian government and the City of Vienna through the strategic project I0. Eurecom's Research is supported in part by its industrial partners: Swisscom, Thales, SFR, Orange, STEricsson, Sharp, BMW Group, Cisco, SAP, Monaco Telecom, and Symantec. This work is also funded in part by the European Commission through the network of excellence Newcom++ and by the Wiener Wissenschafts-, Forschungs-und Technologiefonds (WWTF) through the project PUCCO. The research of Infineon Technologies France is also supported in part by the EU FP7 FET project CROWN.

References

[1] G. S. Smith, "A direct derivation of a single-antenna reciprocity relation for the time domain," *IEEE Transactions on Antennas and Propagation*, vol. 52, no. 6, pp. 1568–1577, June 2004.

[2] A. Bourdoux, B. Côme, and N. Khaled, "Non-reciprocal transceivers in OFDM/SDMA systems: Impact and mitigation," in *Proc. IEEE Radio and Wireless Conference (RAWCON)*, Boston, MA, USA, August 2003, pp. 183 – 186.

[3] M. Guillaud, D. T. Slock, and R. Knopp, "A practical method for wireless channel reciprocity exploitation through relative calibration," in *Proc. Intl. Symposium on Signal Processing and its Applications (ISSPA '05)*, Sydney, Australia, Aug. 2005.

[4] M. Guillaud and F. Kaltenberger, "Exploitation of reciprocity in measured MIMO channels," in *IEEE International Communications Conference (ICC)*, Cape Town, South Africa, May 2010, submitted.

[5] F. Kaltenberger, M. Kountouris, D. Gesbert, and R. Knopp, "On the trade-off between feedback and capacity in measured MU-MIMO channels," *IEEE Trans. Wireless Commun.*, vol. 8, no. 9, pp. 4866–4875, Sep. 2009.

[6] S. Kay, "A fast and accurate sigle frequency estimator," *IEEE Transactions on Acoustic, Speech and Signal Processing*, vol. 37, no. 12, pp. 1987–1990, December 1989.

[7] S. Van Huffel, "Analysis of the total least squares problem and its use in parameter estimation," Ph.D. dissertation, Katholieke Universiteit Leuven, Leuven, Belgium, 1987.

[8] I. Markovsky and S. V. Huffel, "Overview of total least-squares methods," *Signal Processing*, vol. 87, pp. 2283–2302, 2007.

[9] N. Mastronardi, P. Lemmering, and S. van Huffel, "Fast structured total least squares algorithm for solving the basic deconvolution problem," *SIAM Journal on Matrix Analysis and Applications*, vol. 22, 2000.

[10] Y. Hara, Y. Yano, and H. Kubo, "Antenna array calibration using frequency selection in OFDM/SDMA systems," in *Proc. of Globecom'08*, December 2008.

[11] A. Paulraj, D. Gore, and R. Nabar, *Introduction to Space-Time Wireless Communications*. Cambridge University Press, 2003.